

EVOLUTION OF FIELD SPIRAL GALAXIES UP TO REDSHIFTS $Z = 1$ ¹ASMUS BÖHM^{2,3} AND BODO L. ZIEGLER²
Draft version December 2, 2024

ABSTRACT

We have gained intermediate-resolution spectroscopy with the FORS instruments of the Very Large Telescope and high-resolution imaging with the Advanced Camera for Surveys aboard *HST* of a sample of 220 field spiral galaxies within the FORS Deep Field and William Herschel Deep Field. Spatially resolved rotation curves were extracted and fitted with synthetic velocity fields that take into account all geometric and observational effects, like blurring due to the slit width and seeing influence. Using these fits, the maximum rotation velocity V_{\max} could be determined for 124 galaxies that cover the redshift range $0.1 < z < 1.0$ and comprise a variety of morphologies from early-type spirals to very late-types and irregulars. The Tully-Fisher relation (TFR) of this sample, which represents an average look-back time of ~ 5 Gyrs, is offset from the relation of local low-mass spirals, whereas the distant high-mass spirals are compatible with the local TFR. Taking the magnitude-limited character of our sample into account, we show that the slope of local and distant relation would be consistent only if the TFR scatter evolved by more than a factor of 3 between $z \approx 0.5$ and $z \approx 0$. Furthermore, we find that the fraction between stellar and total mass remained constant since $z = 1$, as would be expected in the context of hierarchically growing structure.

Subject headings: galaxies: evolution — galaxies: kinematics and dynamics — galaxies: spiral

1. INTRODUCTION

The concept of Cold Dark Matter (CDM) and its prediction of hierarchical structure growth has become an astrophysical paradigm in the last decade. Observations of the Cosmic Microwave Background (e.g. Spergel et. al 2003) or the Large Scale Structure (e.g. Bahcall et al. 1999) strongly support the idea that the vast majority of matter is non-baryonic, non-luminous and interacts only gravitationally. In this picture, gas and stars are embedded in Dark Matter halos, and low-mass systems were the first virialized structures in the early cosmic stages, followed by an epoch of accretion and merger events during which larger systems were successively built up.

For the case of late-type galaxies, this scenario is supported by, e.g., the observed increasing fraction of disturbed morphologies and merger events towards larger look-back times (e.g. van den Bergh 2002), or the decreasing disk sizes with increasing redshift (e.g. Giallongo et al. 2000; Ferguson et al. 2004). The properties of early-type galaxies, on the other hand, can also be explained with the alternative “monolithic collapse model” of an initial star burst at high redshift that is followed by quiescent evolution (e.g. Sandage 1986).

An important tool for the quantitative test of the predictions from numerical simulations based on the hierarchical scenario are scaling relations that link galaxy parameters. Within the last years, several studies focused on the evolution of such relations up to redshifts $z \approx 1$ — corresponding to more than half the age of the universe — or even beyond. Many analyses utilized the Tully-Fisher Relation (TFR) between the maximum rotation velocity V_{\max} and the luminosity (e.g. Vogt 2001; Ziegler et al. 2002; Milvang-Jensen et al. 2003; Böhm et al. 2004; Bamford et al. 2005; Conselice et al. 2005) or the correlation between luminosity and disk size (e.g. Barden et al. 2004). The results of

these studies were, however, discrepant in some respects. E.g., some studies point towards much higher luminosities of spiral galaxies in the past (e.g. Böhm et al. 2004; Bamford et al. 2005) while others find only a very modest evolution in luminosity (Vogt 2001).

Interestingly, an increasing number of studies point towards a mass-dependent evolution of distant galaxies in terms of their colors (e.g. Kodama et al. 2004), mass-to-light ratios (e.g. van der Wel et al. 2005), or average stellar ages (e.g. Ferreras et al. 2004). The observations indicate that the stellar populations of distant high-mass galaxies are older than those of distant low-mass galaxies, similar to what has been found in the local universe (e.g. Bell & de Jong 2000). Since small galaxies are understood as ancient building blocks within the framework of hierarchical structure growth, and in turn should have an older stellar content than larger systems formed more recently, these observations are a challenge to CDM theory. They can be interpreted such that the main occurrence of star formation shifts from high-mass to low-mass galaxies with growing cosmic age, a phenomenon that was termed “down-sizing” by Cowie et al. (1996).

We here show results from our extensive observational study of spiral galaxy evolution over more than 7 Gyr. Please note that the analysis we gave in Böhm et al. (2004) was limited to ground-based imaging and that the new sample presented here contains almost twice as many distant galaxies. Throughout the article, we will assume a flat cosmology with $\Omega_{\lambda} = 0.7$, $\Omega_m = 0.3$ and $H_0 = 70 \text{ km s}^{-1} \text{ Mpc}^{-1}$.

2. VLT SPECTROSCOPY

We selected our targets utilizing the multi-band photometric surveys in the FORS Deep Field (FDF, Heidt et al. 2003) and

¹ Based on observations collected at the European Southern Observatory, Cerro Paranal, Chile (ESO Nos. 65.O-0049, 66.A-0547, 68.A-0013, 69.B-0278B and 70.B-0251A) and observations with the NASA/ESA *Hubble Space Telescope*, PID 9502 and 9908.

² Institut für Astrophysik Göttingen, Friedrich-Hund-Platz 1, 37077 Göttingen, Germany; boehm@astro.physik.uni-goettingen.de, bziegler@astro.physik.uni-goettingen.de

³ Astrophysikalisches Institut Potsdam, An der Sternwarte 16, 14482 Potsdam, Germany; aboehm@aip.de

William Herschel Deep Field (WHDF, Metcalfe et al. 2001). The following criteria were applied: a) total apparent brightness $R < 23''$, b) spectrophotometric type “later” than Sa, based on a photometric redshift catalogue in the case of the FDF (see Bender et al. 2001) or color-color diagrams for the WHDF objects, c) disk inclination angle $i > 40^\circ$ and misalignment angle between apparent major axis and slit direction $\delta < 15^\circ$. The two latter constraints were chosen to limit the geometric distortions of the observed rotation curves. Apart from these limits, our selection was morphologically “blind”. Note also that no selection on emission line strength was performed.

Using the FORS 1 & 2 instruments of the VLT in multi-object spectroscopy mode, we took spectra of a total of 220 galaxies between September 2000 and October 2002. We used a fixed slit width of 1.0 arcsec which resulted in spectral resolutions of $R \approx 1200$ (for the FDF observations, where the grism 600R was used) and $R \approx 1000$ (in the WHDF, with grism 600RI), respectively. Each setup was exposed for a total of 2.5 hours under seeing conditions between 0.43 arcsec and 0.92 arcsec FWHM, with a median of 0.76 arcsec. The spatial sampling in the final spectra was 0.2 arcsec/pixel (FDF) and 0.25 arcsec/pixel (WHDF, after the FORS 2 CCD upgrade).

The data reduction was conducted on single extracted spectra. All reduction steps were performed on the individual exposures before they were finally combined. The typical rms of the dispersion relation fitted for wavelength calibration was 0.04 Å. For 202 of the galaxies, a redshift determination and spectral classification was feasible. The objects range from $z = 0.03$ to $z = 1.49$ with a median $\langle z \rangle = 0.43$ (the redshift distribution of the final sample entering the Tully–Fisher analysis is given in section 4).

3. HST/ACS IMAGING

The HST/ACS observations were carried out during cycles 11 and 12. To cover the $6 \times 6 \text{ arcmin}^2$ sky areas of the FORS and William Herschel Deep Fields, 2×2 mosaics were taken with the Wide Field camera that has a field-of-view of $\sim 200 \times 200 \text{ arcsec}^2$ and a pixel scale of 0.05 arcsec. 4 visits each with a total exposure time of 2360 s (FDF) and 2250 s (WHDF) through the F814W filter were used per quadrant. Each visit was split into two exposures. We kept the resulting frames from the ACS pipeline reduction (including bias subtraction, flatfielding and distortion correction) and used a filtering algorithm to combine the two exposures of each visit and remove the cosmics (for the FDF images, this was kindly done by A. Riffeser and J. Fliri, University Observatory Munich).

The structural parameters of the galaxies were derived with the GALFIT package (Peng et al. 2002). For convolution of the model profiles, a mean Point Spread Function was constructed using ~ 20 unsaturated stars with $I_{814} < 23$ which were normalized to the same central flux and median-averaged. An exponential profile was used to fit the galaxies’ disk components, while a Sérsic profile was taken to model an additional bulge, where detectable. Note that for the analysis presented here, the most important parameters are the inclination, position angle and scale length of the disk. The best-fitting bulge parameters were only used for a raw morphological classification.

We found significant bulge components in only 46 out of 124 galaxies that were reliable for V_{\max} determination (see next section), spanning the range $0.01 \leq B/T \leq 0.53$ (median $\langle B/T \rangle = 0.15$). In terms of a visual classification within the Hubble scheme, our sample comprises all types from Sa spirals

to irregulars.

4. TULLY–FISHER PARAMETERS

Due to the small apparent sizes of the spirals in our sample, the observed rotation curves are heavily blurred. At redshifts of $z \approx 0.5$, the apparent scale lengths are of the same order as the slit width (one arcsec) and the seeing disk. The maximum rotation velocity hence cannot be derived “straightforward” from the outer regions of the observed rotation curves.

To account for these blurring effects, we performed simulations of the slit spectroscopy by generating synthetic rotation velocity fields according to the disk inclination, position angle and scale length of a given object. We assumed an intrinsic linear rise of the rotation velocity which turns over into a regime of constant rotation velocity at large radii, with the turnover radius computed from the scale length of the emitting gas (for details as well as tests of other rotation curve shapes and examples of observed rotation curves, we refer to Böhm et al. 2004). After weighting with the luminosity profile, convolution with the Point Spread Function and extraction of a stripe from the velocity field (the width and position of which corresponded to the slit used for spectroscopy), this simulation yielded a *synthetic* rotation curve which was fitted to the corresponding observed curve to derive the intrinsic value of V_{\max} . Following this approach, V_{\max} values could be determined for 124 spirals in our sample (hereafter TF sample). The remaining 78 galaxies were rejected due to low S/N , disturbed kinematics, solid-body rotation or the lack of significant rotation within the measurement errors. The TF sample galaxies span the redshift range $0.05 < z < 0.97$ (median 0.45, corresponding to a lookback time of 4.7 Gyr) and comprise 19 objects with spectrophotometric type Sab, 65 Sc spirals and 40 Sdm galaxies. V_{\max} values fall in the range $22 \text{ km/s} < V_{\max} < 450 \text{ km/s}$ (median 135 km/s).

The computation of the luminosities benefitted strongly from the multi-band imaging of our targets. Depending on the redshift of a given object, the filter which best matched the rest-frame B-band was used to compute the absolute magnitude M_B . This way, systematic k -correction errors due to dependence on the SED are very small (<0.1 mag for all types and redshifts in our data set). Intrinsic absorption was corrected following Tully & Fouqué (1985). In this approach, the amount of absorption only depends on the disk inclination. For testing purposes, we alternatively applied the inclination- and mass-dependent correction factors given by Tully et al. (1998). However, this did not change the results presented in the following. It only is crucial that any distant sample is corrected for internal absorption *in the same way* as the local sample it is compared to. Since we use the local data from Pierce & Tully (1992) here, who adopted the Tully & Fouqué approach, we will keep this convention in the following. The TF galaxies have absolute magnitudes between $M_B = -16.8$ and $M_B = -22.7$ (median -20.3).

In Fig. 1, we compare our sample to the local Tully–Fisher relation. On average, the FDF & WHDF spirals are more luminous than their local counterparts by $\langle \Delta M_B \rangle = -0.84''$, which could be due to younger stellar populations, i.e. lower M/L ratios of the distant galaxies. This interpretation is supported by the fact that the amount of the distant galaxies’ brightening ΔM_B increases with redshift. A linear χ^2 -fit yields $\Delta M_B = (-1.22 \pm 0.40)z - (0.02 \pm 0.20)[\text{mag}]$ (here, we took the error propagation of V_{\max} errors as well as the typical errors for the local spirals into account). This luminosity evolution is in agreement with the findings by, e.g., Milvang-Jensen et al. (2003),

but exceeds the very modest TF offsets derived by Voigt (2001).

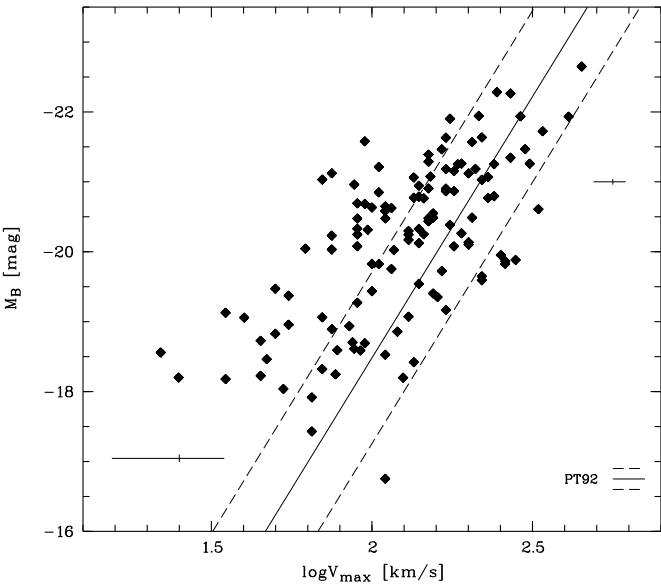


FIG. 1 — The distant FDF & WHDF galaxies at $\langle z \rangle = 0.45$ compared to the local Tully-Fisher relation as given by Pierce & Tully (1992; the dashed lines denote the 3σ limits). The distant spirals are systematically overluminous for their values of V_{\max} . Typical error bars for the high-mass and low-mass regime are indicated in the lower left and upper right corner, respectively.

5. DISCUSSION

The luminosity–rotation velocity distribution of our sample indicates that the offsets from the local Tully–Fisher Relation change not only with redshift but also with mass: while the high-mass spirals are in relatively good agreement with the local TFR, the low-mass spirals are overluminous by up to several magnitudes at given V_{\max} (cf. Fig. 1). Using a 100 iteration bootstrap *bisector* fit, we find an intermediate-redshift TFR of $M_B = -(4.27 \pm 0.18) \log V_{\max} - (11.18 \pm 0.75)$, which is a significantly shallower slope a than locally, where $a = -7.48$ is observed (Pierce & Tully 1992; we emphasize that this published value is in good agreement with a bisector fit to the local sample which yields $a = -7.57 \pm 0.38$). Note that the bisector fitting method — which is a combination of a “forward” and an “inverse” TF fit — can be only weakly affected by potentially correlated errors in ΔM_B and V_{\max} suspected by Bamford et al. (2005).

We reported earlier on a potential mass–dependent luminosity evolution with an analysis that was limited to the FDF sub-sample and ground–based structural parameters (Ziegler et al. 2002; Böhm et al. 2004). Therein, we have shown that the flat distant TFR slope is very unlikely to be introduced by tidally induced star formation in close galaxy pairs, a false assumption on the amount of intrinsic absorption or perturbated/truncated rotation curves. Moreover, we found that the TF slope change holds valid if we sub-divide the sample according to galaxy type or redshift.

We also tested whether a shallower distant TF slope could be mimicked by an incompleteness effect arising from the limit in apparent magnitude due to our target selection. Towards higher redshifts, such a limit corresponds to higher luminosities and, in turn, higher masses. A fraction of the low-luminosity, low-mass (slowly rotating) spiral population is therefore missed in

the selection process, while the low-mass galaxies that are selected may be biased towards TF offsets on the high-luminosity side of the relation. A key factor for the strength of this selection effect is the scatter of the TFR, which locally has a value of 0.41 mag in the B -band. In a previous analysis (Ziegler et al. 2002), we assumed that this scatter increases by a factor of 1.5 between $z \approx 0$ and $z = 0.5$ due to, e.g., a broader distribution in star formation rates at earlier cosmic stages. Here, we will use a different approach by testing *how strongly the TF scatter would have to evolve over the past ~ 5 Gyr for the V_{\max} -dependent TF offsets to be attributed to an incompleteness effect*. We will hence assume that the slope of the TFR remains constant over the redshift range under scrutiny here, and that its scatter has been larger at earlier cosmic times. Similar to the technique described by Giovanelli et al. (1997), we used a comparison between the observed luminosity function of our sample and the Schechter LF form to quantify the incompleteness towards the faint end of the luminosity distribution. The characteristic luminosity M^* and the space density ϕ^* were fitted to the (complete) bright end of the observed distribution, while a fixed faint end index $\alpha = -1.2$ was assumed. The fraction between the number density per unit magnitude of the observed LF and the Schechter LF defined an incompleteness function y that ranged from 1 in the case of completeness to 0 in the case of total incompleteness. On the basis of a given *local* TFR ($M_B = -7.48 \log V_{\max} - 3.52$) with scatter σ and the observed *distant* V_{\max} values and corresponding incompleteness function values of each galaxy, a simulated TFR sample was constructed. This simulation was repeated 800 times and the resulting synthetic sample was fitted using a bootstrap bisector algorithm. The whole procedure was used to quantify the incompleteness effect and to de-bias the observed TFR. Note that the de-biased M_B magnitudes are fainter than the observed values and that the TFR becomes steeper after de-biasing.

This way, we found that the distant TFR slope is $a = -5.01 \pm 0.28$ if the distant TF scatter was the same as locally. If the scatter doubles between $z = 0$ and $z \sim 0.5$, the incompleteness effect becomes stronger and the de-biased distant TFR slope would be $a = -6.78 \pm 0.30$. Assuming a three times larger scatter than locally we found a de-biased distant slope of $a = -7.72 \pm 0.32$. Note that the local TFR is *also* affected by a magnitude limit. The de-biased local TF bisector fit slope we find is $a = -8.02 \pm 0.41$ (here, the unchanged local TF scatter of $\sigma_B = 0.41^m$ was kept). We hence conclude that the distant and local TFR would be consistent in terms of an incompleteness effect *if the TF scatter evolved by more than a factor of 3 over the past ~ 5 Gyr*. This would be in agreement with the observed distant scatter which is $\sigma \approx 1.2$ mag. On the other hand, this might be an overestimate since the free-fit scatter (i.e., with a slope $a = -4.27$, see beginning of this section) is only ~ 0.9 mag.

Though these results imply that the distant TF distribution can at least in part be attributed to an incompleteness effect, we emphasize that an analysis with single-zone models of the broad-band colors of 30 galaxies from our data set yielded evidence for a dependence of the mean stellar ages on V_{\max} (i.e. mass): the high-mass galaxies have older stellar populations than the low-mass ones (see Ferreras et al. 2004). This indication for an anti-hierarchical evolution of the baryonic component of galaxies (“down-sizing”) has also been found in other studies of distant galaxies (e.g. Kodama et al. 2004; van der Wel et al. 2005). It is possible that the various evolutionary effects

coming into play between the earlier and the local universe — the evolution of the stellar populations and gas fractions, disk growth etc. — balance each other in such a way that the down-sizing phenomenon is *not* reflected in a significant differential evolution of the Tully–Fisher Relation.

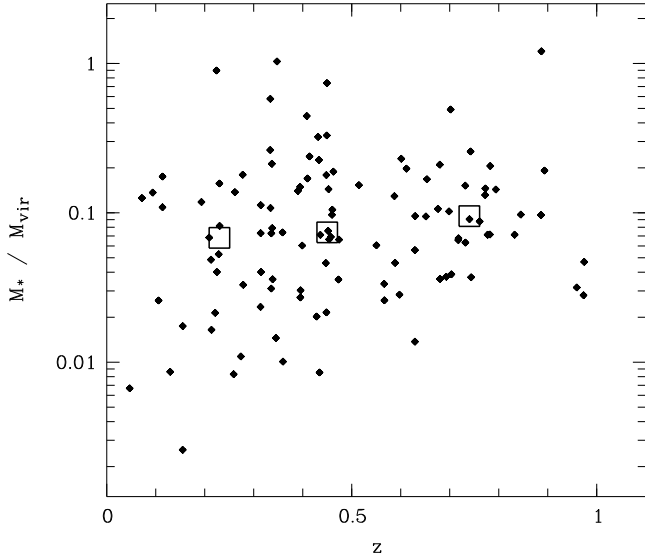


FIG. 2 — Stellar-to-total mass fraction of 110 galaxies from our sample with determined V_{\max} and K -band photometry available. The three large open squares show the median mass fraction within three redshift bins containing 36–37 galaxies each. The lack of a stellar mass fraction increase towards lower redshift favours a hierarchical buildup of the galaxies (see text for details).

Using a similar approach as Conselice et al. (2005), we now want to focus on the evolution of the ratio between stellar and total mass since $z = 1$. K -band data are available for 110 objects from the TF sample. Computing the rest-frame, absorption-corrected $B-R$ index of our sample galaxies, and adopting the local correlation between $B-R$ and K -band M/L ratio given by Bell & de Jong (2001), we transformed the absolute K magnitudes into stellar masses M_* . Total masses were estimated on the basis of the disk scale length and maximum rotation velocity following van den Bosch (2002). Our sample covers the ranges $2.0 \cdot 10^8 M_{\odot} < M_* < 3.7 \cdot 10^{11} M_{\odot}$ (median $9.0 \cdot 10^9 M_{\odot}$) in stellar mass and $2.5 \cdot 10^9 M_{\odot} < M_{\text{vir}} < 5.2 \cdot 10^{12} M_{\odot}$ (median

$1.1 \cdot 10^{11} M_{\odot}$) in total mass.

In Fig. 2, we show the ratio between stellar and total mass as a function of redshift. If we sub-divide our sample into three redshift bins with 36 to 37 galaxies in each bin, we find median stellar mass fractions of 0.068, 0.074 and 0.095 at redshifts $z < 0.35$, $0.35 < z < 0.6$ and $z > 0.6$, respectively. We hence do not find evidence for an increase of the stellar mass fraction of spirals between $z = 1$ and the local universe which would be expected if the galaxies contained all their gas by redshift unity and only conversion of gas into stars took place since then. Instead of such a “monolithic” scenario — which can be used to describe the evolution of massive ellipticals —, the data indicate that spiral galaxies have accreted baryonic (and most probably also dark) matter in the regime $0 < z < 1$, in agreement with the observational findings of Conselice et al. (2005).

6. CONCLUSIONS

We have used VLT/FORS spectroscopy and HST/ACS imaging to construct a sample of 220 field spiral galaxies up to redshift $z = 1$. Spatially resolved rotation curves were extracted and fitted with synthetic velocity fields that take into account all geometric and observational effects, like blurring due to the slit width and seeing influence. Using these fits, the maximum rotation velocity V_{\max} could be determined for 124 galaxies. The Tully–Fisher relation of this sample, which represents an average look-back time of ~ 5 Gyrs, is offset from the relation of local low-mass spirals, whereas the distant high-mass spirals are compatible with the local TFR. Taking the magnitude-limited character of our sample into account, we have shown that the slope of local and distant relation would be consistent only if the TFR scatter evolved by more than a factor of 3 between $z \approx 0.5$ and $z \approx 0$. Furthermore, we found that the fraction between stellar and total mass remained constant since $z = 1$, as would be expected in the context of hierarchically growing structure.

We thank ESO for the efficient support during the spectroscopic observations and the FDF Team for the contributions to the first analysis of the FDF sub-sample. We also are grateful to J. Heidt (LSW Heidelberg) for taking pre-images of the WHDF and N. Metcalfe (Durham) for providing data on the WHDF photometry. This work was funded by the Volkswagen Foundation (I/76520) and the “Deutsches Zentrum für Luft- und Raumfahrt” (50OR0301).

REFERENCES

Bahcall, N., Ostriker, J. P., Perlmutter, S., & Steinhardt, P. J. 1999, *Science*, 284, 1481
 Bamford, S. P., Aragon-Salamanca, A., Milvang-Jensen, B. 2005, *MNRAS*, in press (astro-ph/0511442)
 Barden, M., Rix, H.-W., Somerville, R. S., et al. 2005, *ApJ*, 635, 959
 Bell, E. F., & de Jong, R. S. 2000, *MNRAS*, 312, 497
 Bell, E. F., & de Jong, R. S. 2001, *ApJ*, 550, 212
 Bender, R., Appenzeller, I., Böhm, A., et al. 2001, in ESO astrophysics symposia, Deep Fields, ed. S. Cristiani, A. Renzini, & R. E. Williams, (Springer), 96
 Böhm, A., Ziegler, B. L., Saglia, R. P., et al. 2004, *A&A*, 420, 97
 Conselice, C. J., Bundy, K. E., Richard, S., Brichmann, J., Vogt, N. P., Phillips, A. C. 2005, *ApJ*, 628, 160
 Cowie, L. L., Songaila, A., Hu, E. M., Cohen, J. G. 1996, *AJ*, 112, 839
 Ferguson, H. C., Dickinson, M., Giavalisco, M., et al. 2004, *ApJ*, 600, 107
 Ferreras, I., Silk, J., Böhm, A., & Ziegler, B. L. 2004, *MNRAS*, 355, 64
 Giallongo, E., Menci, N., Poli, F., D’Odorico, S., & Fontana, A. 2000, *ApJ*, 530, L73
 Giovanelli, R., Haynes, M. P., Herter, T., et al. 1997, *AJ*, 113, 53
 Heidt, J., Appenzeller, I., Gabasch, A., et al. 2003, *A&A*, 398, 49
 Kodama, T., Yamada, T., Akiyama, M., et al. 2004, *MNRAS*, 350, 1005
 Metcalfe, N., Shanks, T., Campos, A., McCracken, H. J., & Fong, R. 2001, *MNRAS*, 323, 779
 Milvang-Jensen, B., Aragón-Salamanca, A., Hau, G. K. T., Jørgensen, I., & Hjorth, J. 2003, *MNRAS*, 339, L1
 Peng, C. Y., Ho, L. C., Impey, C. D., & Rix, H.-W. 2002, *AJ*, 124, 266
 Pierce, M. J., & Tully, R. B. 1992, *ApJ*, 387, 47
 Sandage, A. 1986, *A&A*, 161, 89
 Spergel, D. N., Verde, L., Peiris, H. V., et al. 2003, *ApJS*, 148, 175
 Tully, R. B., & Fouqué, P. 1985, *ApJS*, 58, 67
 Tully, R. B., Pierce, M. J., Huang, J.-S., et al. 1998, *AJ*, 115, 2264
 van den Bergh, S. 2002, *PASP*, 114, 797
 van den Bosch, F. C. 2002, *MNRAS*, 332, 456
 van der Wel, A., Franx, M., van Dokkum, P. G., Rix, H.-W., Illingworth, G. D., & Rosati, P. 2005, *ApJ*, 631, 145
 Vogt, N. P. 2001, in ESO astrophysics symposia, Deep Fields, ed. S. Cristiani, A. Renzini, & R. E. Williams, (Springer), 112
 Ziegler, B. L., Böhm, A., Fricke, K. J., et al. 2002, *ApJ*, 564, L69